Chinese Herbal Medicines 14 (2022) 273–282

Contents lists available at ScienceDirect

Chinese Herbal Medicines

journal homepage: www.elsevier.com/locate/chmed

Original Article

Network pharmacology analysis to explore mechanism of Three Flower Tea against nonalcoholic fatty liver disease with experimental support using high-fat diet-induced rats

Peixuan Wu [a], Shufei Liang [a], Yanping He [a], Rui Lv [a], Bendong Yang [a], Meng Wang [a], Chao Wang [a], Yong Li [c], Xinhua Song [a,b,*], Wenlong Sun [a,b,*]

[a] Institute of Biomedical Research, School of Life Sciences and Medicine, Shandong University of Technology, Zibo 255000, China
[b] Shandong Qingyujiangxing Biotechnology Co., Ltd., Zibo 255000, China
[c] Shandong Tianyin Biotechnology Co., Ltd., Zibo 255000, China

ARTICLE INFO

Article history:
Received 19 May 2021
Revised 12 September 2021
Accepted 18 October 2021
Available online 12 March 2022

Keywords:
network pharmacology
nonalcoholic fatty liver disease
Three Flower Tea

ABSTRACT

Objective: Nonalcoholic fatty liver disease (NAFLD) has become a common chronic liver disease that is harmful to human health. Moreover, there is currently no FDA-approved first-line drug for the treatment of nonalcoholic steatohepatitis (NASH) or NAFLD. Traditional Chinese medicine (TCM) is widely used to ameliorate liver diseases, such as the traditional ancient recipe called Three Flower Tea (TFT), which consists of double rose (*Rosa rugosa*), white chrysanthemum (*Chrysanthemum morifolium*), and Daidaihua (*Citrus aurantium*). However, the mechanisms of the action of TFT are not clear. Therefore, this study aimed to elucidate the mechanisms of TFT against NAFLD in high-fat diet (HFD)-induced rats.

Methods: This study utilized bioinformatics and network pharmacology to establish the active and potential ingredient-target networks of TFT. Furthermore, a protein–protein interaction (PPI) network was constructed, and enrichment analysis was performed to determine the key targets of TFT against NAFLD. Furthermore, an animal experiment was conducted to evaluate the therapeutic effect and confirm the key targets of TFT against NAFLD.

Results: A total of 576 NAFLD-related genes were searched in GeneCards, and under the screening criteria of oral bioavailability (OB) ≥30% and drug-likeness (DL) ≥0.18, a total of 19 active ingredients and 210 targets were identified in TFT. Network pharmacology analysis suggested that 55 matching targets in PPIs were closely associated with roles for NAFLD treatment. Through the evaluation of network topology parameters, four key central genes, *PPARγ*, *SREBP*, *AKT*, and *RELA*, were identified. Furthermore, animal experiments indicated that TFT could reduce plasma lipid profiles, hepatic lipid profiles and hepatic fat accumulation, improve liver function, suppress inflammatory factors, and reduce oxidative stress. Through immunoblotting and immunofluorescence analysis, PPARγ, SREBP, AKT, and RELA were confirmed as targets of TFT in HFD-induced rats.

Conclusion: In summary, our results indicate that TFT can prevent and treat NAFLD via multiple targets, including lipid accumulation, antioxidation, insulin sensitivity, and inflammation.

1. Introduction

Nonalcoholic fatty liver disease (NAFLD), a continuum of liver abnormalities from nonalcoholic fatty liver (NAFL) to nonalcoholic steatohepatitis (NASH), has a variable course and can lead to cirrhosis and liver cancer (Marrero et al., 2002; Rinella & Sanyal, 2015). There has been an increase in NAFLD prevalence, paralleling a worldwide increase in diabetes and metabolic syndrome. Up to 30% of the general population and 75% of obese individuals are diagnosed with this disease (Amarapurkar et al., 2007). Patients with NAFLD experience symptoms such as poor digestion, physical weakness, dull pain in the liver area, and hepatosplenomegaly. Moreover, these symptoms are usually accompanied by obesity, overweight, diabetes, and metabolic syndrome, and a small number of patients develop liver fibrosis or liver cirrhosis (Kumar,

* Corresponding authors.
E-mail addresses: 892442572@qq.com (X.h. Song), 512649113@qq.com (W.I. Sun).

https://doi.org/10.1016/j.chmed.2022.03.002
1674-6384/

2013). Changing lifestyles, strengthening physical exercises, and reducing weight are effective ways to prevent and treat this disease, but few people can maintain weight loss for a sustained period (Thoma, Day, & Trenell, 2012). Patients still rely on adjuvant drugs for treatment; however, currently, some therapeutic drugs that have not yet received FDA approval have emerged (Caldwell, Argo, & Alosaimi, 2006). Therefore, people urgently need a safe and effective drug to assist in the treatment of NAFLD.

After thousands of years of clinical use, traditional Chinese medicines (TCMs) have been widely used to treat various diseases and has gradually been recognized by an increasing number of people worldwide due to its few side effects and remarkable curative effects (Chen, 2012). Three Flower Tea (TFT), which consists of double rose (*Rosa rugosa* Thunb.), white chrysanthemum (*Chrysanthemum morifolium* Ramat.), and Daidaihua (*Citrus aurantium* L.), has been a type of TCMs since ancient times and might be beneficial for preventing and treating NAFLD. However, due to the multiple and sophisticated pathogenesis of NAFLD, we still do not clearly know the efficacy and mechanism of TFT for NAFLD prevention and treatment (Friedman et al., 2018).

Network pharmacology is a new method developed on the basis of the theory of an "active ingredient, target and disease" interactive network (Hopkins, 2008). Based on the perspective of systems science, the role of network intervention and TCMs in the treatment of diseases has been studied. The integration and system-level perspective of network pharmacology research strategies are consistent with the holistic concept and dialectical treatment theory of TCMs, which provides a novel way for modern medicine to interpret the system-level effects of TCMs. In this study, we evaluated the mechanism of TFT against NAFLD using bioinformatic and network pharmacology methods. Furthermore, we verified the main mechanisms and key targets of TFT against NAFLD in high-fat diet (HFD)-induced rats.

2. Materials and methods

2.1. NAFLD target identification

To predict disease targets, the key word "NAFLD" was used in the GeneCards database (https://www.genecards.org) to search for NAFLD-related targets. After collecting all relative targets in GeneCards, we used the online tool String (https://string-db.org/) to transform all targets into targets in humans.

2.2. Identification of ingredients and targets of TFT

The Traditional Chinese Medicine System Pharmacology Database (TCMSP, https://tcmspw.com/tcmsp.php) was used to identify the ingredients in double rose, white chrysanthemum, and Daidaihua. The active compounds were filtered according to oral bioavailability (OB) and drug-likeness (DL) values, and the components were preserved if the OB $\geq$30% and the DL $\geq$0.18. Moreover, we collected potential targets of each ingredient in the TCMSP database. Furthermore, Cytoscape 3.6.0 software was used to show the interactions between herbs and active components.

2.3. Prediction of TFT targets for NAFLD treatment

Perl (5.30) was used to overlap the NAFLD targets obtained from GeneCards and the potential targets of TFT ingredients to obtain the potential NAFLD-related targets of TFT. Furthermore, the TFT ingredient-NAFLD target network was constructed by using Cytoscape.

2.4. Functional enrichment and pathway enrichment analysis

Gene ontology (GO) enrichment, which includes biological processes, molecular functions and cellular components, and Kyoto Encyclopedia of Genes and Genomes (KEGG) pathway enrichment were performed and visualized by the "ClusterProfiler" package in R version 4.0.2.

2.5. Construction and analysis of protein–protein interaction (PPI) network

The PPI background was obtained from the Human Protein Reference Database (https://www.hprd.org). A PPI network of the potential targets in TFT for NAFLD treatment was constructed by Cytoscape and clustered by the clusterMaker app in Cytoscape. The degree value and the topological parameters of nodes in networks were evaluated using NetworkAnalyzer. A higher degree value node represented crucial targets in the PPI network.

2.6. Animal experiments

The rats (8 weeks, 200 ± 20 g) were purchased from Shandong Animal Experiment Center (Jinan, China) with the permission number SCXK 2014–0007. The rats were housed at (25 ± 0.5) °C under a 12 h light/dark cycle for adaptation for one week. All animal procedures were performed in accordance with the Guidelines for Care and Use of Laboratory Animals of Shandong University of Technology and permitted by the Animal Ethics Committee of Shandong University of Technology. The rats were randomly divided into three groups (n = 8 per group). The rats fed standard chow and normal drinking water were set as the normal control (NC) group. The rats fed HFD chow (D12451, SYSE Company, Changzhou, Jiangsu, China) and normal drinking water were set as the HFD control (HC) group. The rats fed HFD chow and drinking water containing 1.5% TFT extract were set as the TFT treatment (TF) group (Woods et al., 2003). TFT extract was freshly prepared daily. To prepare the 1.5% TFT extract solution, 1.5 g of TFT (white chrysanthemum, double rose and Daidaihua = 2:1:2) was suspended in 100 mL of hot water (85 °C), brewed for 5 min, cooled to room temperature and filtered (Kou et al., 2005). During the last week, the body weights and food intake in each group were recorded. All rats were sacrificed, and blood samples were acquired and subsequently centrifuged at 3000 rpm for 5 min at 4 °C to obtain plasma, which was then preserved at −80 °C until further analysis. Liver samples were also collected, frozen with liquid nitrogen and stored at −80 °C.

2.7. Measurement of biochemical index in plasma

Plasma and liver samples were used to determine biochemistry parameter levels, including total cholesterol (TC) and triglycerides (TGs), in both plasma and liver and low-density lipoprotein cholesterol (LDL-C) and high-density lipoprotein cholesterol (HDL-C) levels in plasma. These parameters were measured immediately using corresponding kits from Jiancheng Bioengineering Institute (Nanjing, Zhejiang, China). In addition, plasma alanine aminotransferase (ALT) and aspartate aminotransferase (AST) levels were also

determined directly using commercial kits (Nandi, Patra, & Swarup, 2006).

2.8. Haematoxylin and eosin (HE) staining

HE staining was performed to observe the degree of fat accumulation in the liver. The liver tissue was infiltrated with formalin, embedded in paraffin, cut into 3-μm thick sections, stained with HE, and then observed with a light microscope at 40 times magnification (Adler & Schaffner, 1979).

2.9. Immunofluorescence

The liver tissues were plated on coverslips and sliced into 3-μm sections. The sections were fixed with 4% paraformaldehyde for 20 min. After washing three times with PBS, the sections were permeabilized with 1% Triton X-100 in PBS for 30 min. These sections were incubated with primary antibodies against SREBP1 (K106528P, Solarbio Company), p65 NF-κB (K200045M, Solarbio Company, Beijing, China), and PPARγ (K001647P, Solarbio Company, Beijing, China) overnight at 4 °C. Subsequently, the cells were washed three times with PBS and incubated with FITC-labelled goat anti-rabbit secondary antibody. The nuclei were stained with 6-diamidino-2-phenylindole (DAPI). Finally, the sections were observed under a microscope (Harry, Pogliano, & Losick, 1995).

2.10. Western blot analysis

For the Western blot experiments, total proteins in liver tissue were lysed for 30 min using ice-cold RIPA lysis buffer. The lysates were then collected after centrifugation at 4 °C for 15 min at 12 000 g. The protein concentration was measured by bicinchoninic acid (BCA) assay (Thermo Fisher Scientific, Beijing, China). Equal amounts (20 μg) of protein fractions were separated by electrophoresis on 12% sodium dodecyl sulfate (SDS)-polyacrylamide gel electrophoresis (PAGE) gels and then transferred to polyvinylidene difluoride (PVDF) membranes. The membranes were blocked with 5% (mass-to-volume ratio) nonfat milk powder in Tris-buffered saline containing 0.1% (volume percent) Tween-20 (TBST) and then incubated overnight with primary antibodies [anti-AKT1 antibody (K101311P, 1:1000) and anti-pAKT antibody (K006214P, 1:1000) purchased from Solarbio Company, Beijing, China] at 4 °C. Subsequently, the membranes were washed three times with TBST for 10 min each time. After washing, the blots were further incubated with secondary antibodies diluted 1:2000, including horseradish peroxidase (HRP)-conjugated goat anti-rabbit for 2 h at room temperature. After additional washing, HRP activity was detected by enhanced chemiluminescence (ECL) according to the manufacturer's instructions. The experiment was repeated three times (Gierke et al., 2004).

2.11. Statistical analysis

In this experiment, we employed GraphPad Prism 8 software to determine the mean ± standard deviation of the results from each experiment. Differences were considered significant at $^{*}P < 0.05$, $^{**}P < 0.01$, and $^{***}P < 0.001$ according to One-way ANOVA with LSD post hoc test for multiple comparisons (Mavrevski et al., 2018).

3. Results

3.1. NAFLD target identification

All NAFLD targets were searched in the GeneCards database with the key word "NAFLD", and 576 genes were identified after transformation into the *Homo sapiens* group on the String website (Table S1). These targets were associated with approved drugs and integrated from expert curated repositories, GWAS catalogues, animal models and the scientific literatures.

3.2. Ingredients and targets of TFT

We searched double rose, white chrysanthemum, and Daidaihua in TCMSP and collected the ingredients and potential targets of each herb. Under the conditions of OB > 30% and DL > 0.18, for double rose, the numbers of ingredients and active targets were six and 161, respectively. For Daidaihua, the numbers of ingredients and active targets were four and 39, respectively. For white chrysanthemum, the numbers of ingredients and active targets were 13 and 207, respectively (Fig. 1A). After the removal of duplicate ingredients and potential targets, a total of 19 ingredients and 210 targets were identified. The detailed results are shown in Table S2.

3.3. Ingredient-target-disease network of TFT

According to the intersection of NAFLD targets and potential targets of TFT, the ingredient-target-disease network of TFT was constructed and shown in Fig. 1B and Table S3. In detail, white chrysanthemum contained six active ingredients, double rose contained three active ingredients, and Daidaihua contained two active ingredients. Moreover, white chrysanthemum and double rose had two common active ingredients, while Daidaihua and white chrysanthemum have two common active ingredients. Furthermore, with regard to targets, there were nine genes targeted by all three herbs, 33 genes targeted by both white chrysanthemum and double rose, and eight genes targeted by both white chrysanthemum and Daidaihua. There were three genes targeted by white chrysanthemum alone and two genes targeted by double rose alone.

3.4. Functional enrichment analysis

To elucidate the multiple biological functions of potential targets of TFT in NAFLD, GO enrichment analysis was performed (Figs. S1–S3). For biological processes, the potential targets of TFT were enriched in response to nutrient levels, response to lipopolysaccharide, response to molecules of bacterial origin, etc. (Fig. S1 and Table S4). For cellular components, the potential targets of TFT were significantly enriched in membrane rafts, membrane microdomains, membrane regions, etc. (Fig. S2 and Table S5). RNA polymerase II-specific DNA-binding transcription factor binding, nuclear receptor activity, ligand-activated transcription factor activity, etc., were particularly enriched in molecular functions (Fig. S3 and Table S6). Furthermore, KEGG pathway enrichment analysis was shown in Fig. S4 (the top 20 pathways) and Table S7. The fluid shear stress and atherosclerosis pathway (hsa05418), AGE–RAGE signalling pathway in diabetic complications (hsa04933), TNF signalling pathway (hsa04668), IL-17 signalling pathway (hsa04657), and NAFLD pathway (hsa04932) were the top 5 significantly impacted pathways.

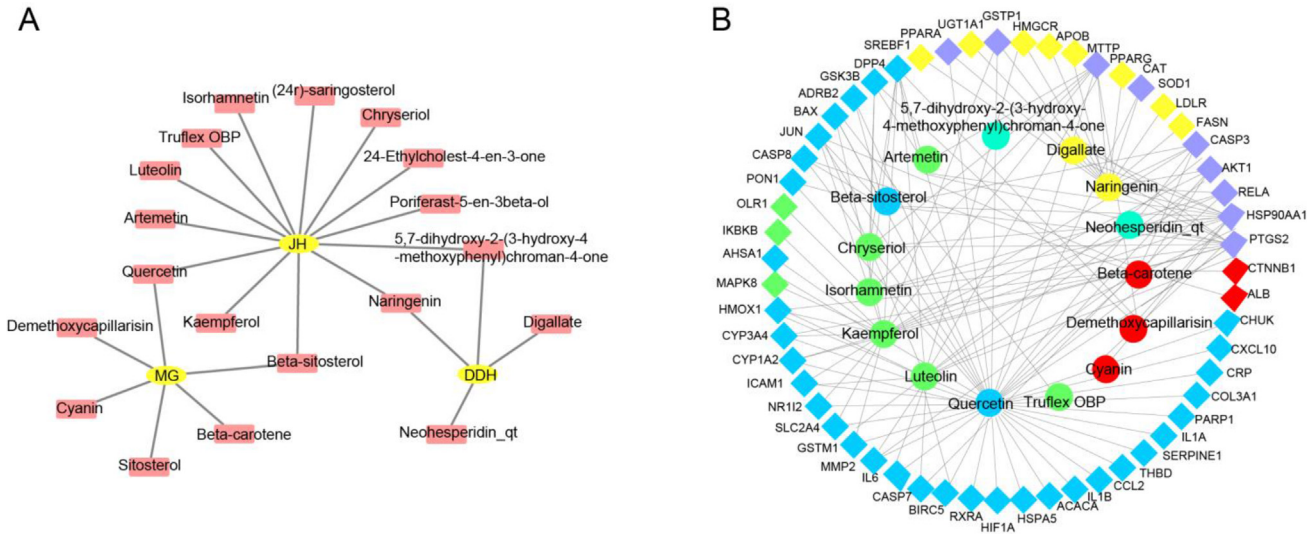

Fig. 1. Herb-ingredient-target-disease network of TFTs for NAFLD prevention and treatment. A: The herb-ingredient network of TFT; B: the ingredient-target-disease network of TFT. Purple represents the genes targeted by all three herbs, yellow represents genes targeted by both Daidaihua and white chrysanthemum, and blue represents genes targeted by both white chrysanthemum and double rose. Light green represents genes targeted by Daidaihua, dark green represents genes targeted by white chrysanthemum, and red represents genes targeted by double rose.

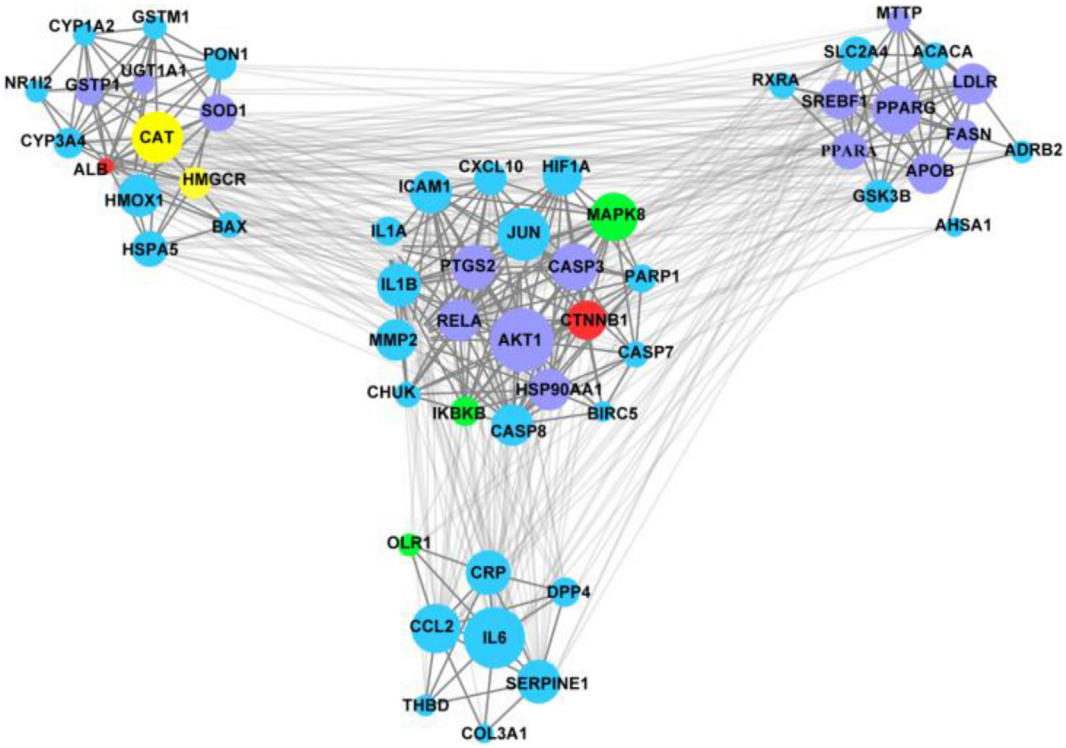

Fig. 2. PPI network of TFT for NAFLD prevention and treatment. Circles represent ingredients, and prisms represent genes. Purple represents the three types of herbs, yellow represents Daidaihua and white chrysanthemum, and blue represents white chrysanthemum and double rose. Light green represents Daidaihua, dark green represents white chrysanthemum, and red represents double rose.

3.5. PPI network analysis

The PPI network is shown in Fig. 2; there were 55 nodes and 545 edges. The connecting pieces were clustered by clusterMaker, and the degree value of nodes was calculated by NetworkAnalyzer. The larger the degree value is, the larger the corresponding node. Therefore, in the PPI network, the *AKT1*, *IL-6*, *PPARG*, *SREBF1* and *RELA* genes with degree values ≥20 were identified as major nodes.

3.6. Effect of TFT on body weight, food intake, blood glucose, and plasma lipid profiles in HFD-induced rats

As shown in Fig. 3A–C, compared with the NC group, the HC group showed a significant increase in body weight ($P < 0.001$) and a significant decrease in food intake ($P < 0.001$), while the blood glucose levels of both groups remained similar. Compared with the HC group, the TF group showed similar levels of body

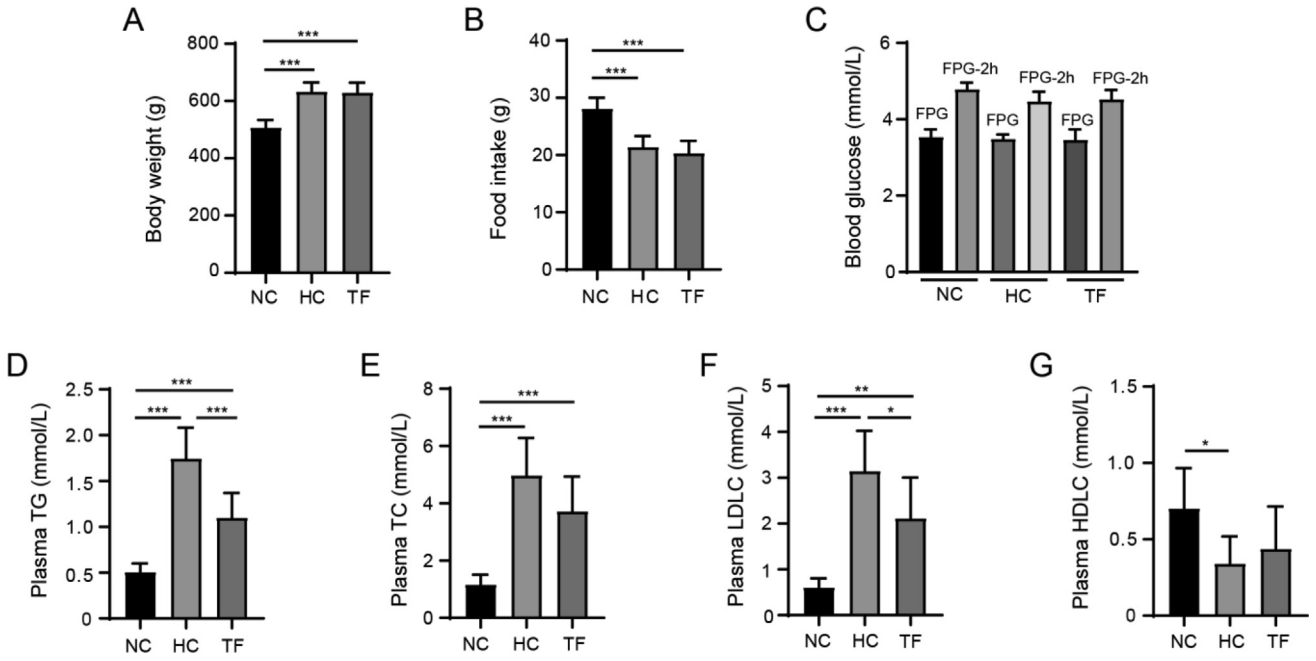

Fig. 3. Effect of TFT on body weight (A), food intake (B), blood glucose (C), and plasma lipid profiles (D–G) in HFD-induced rats (mean SD, $n = 6$). NC: rats fed standard chow and provided normal drinking water; HC: rats fed HFD chow and provided normal drinking water; TF: rats fed HFD chow and drinking water containing 1.5% TFT. Significant differences were observed at $^{*}P < 0.05$, $^{**}P < 0.01$, $^{***}P < 0.001$ by using One-way ANOVA with LSD post hoc test for multiple comparisons.

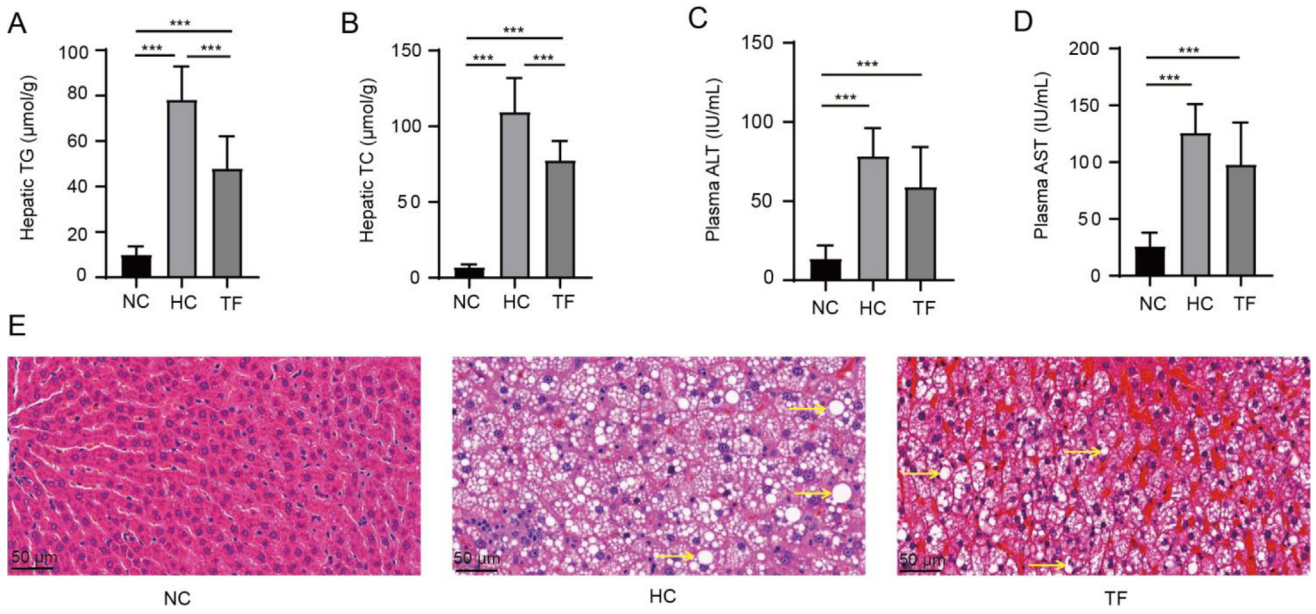

Fig. 4. Effect of TFT on hepatic lipid profiles, liver function, and hepatic histomorphology in HFD-induced rats. A: Hepatic TG; B: hepatic TG; C: plasma ALT; D: plasma AST; E: HE staining of liver tissue. Scale bars: 50 μm. Arrows point to lipid droplets.

weight, food intake, and blood glucose. Furthermore, as shown in Fig. 3D–G, compared with the NC group, the HC group showed significant increases in TG ($P < 0.001$), TC ($P < 0.001$), and LDLC ($P < 0.001$) levels and a significant decrease in HDLC ($P < 0.05$) levels. Compared with the HC group, the TF group showed significant decreases in TG ($P < 0.001$) and LDLC ($P < 0.05$). Although compared with the HC group, the TC and HDLC levels of the TF group did not change substantially, the TC of the TF group still exhibited a decrease ($P = 0.0629$), which might indicate that TFT mainly functions to lower TC, TG, and LDLC but cannot raise HDLC.

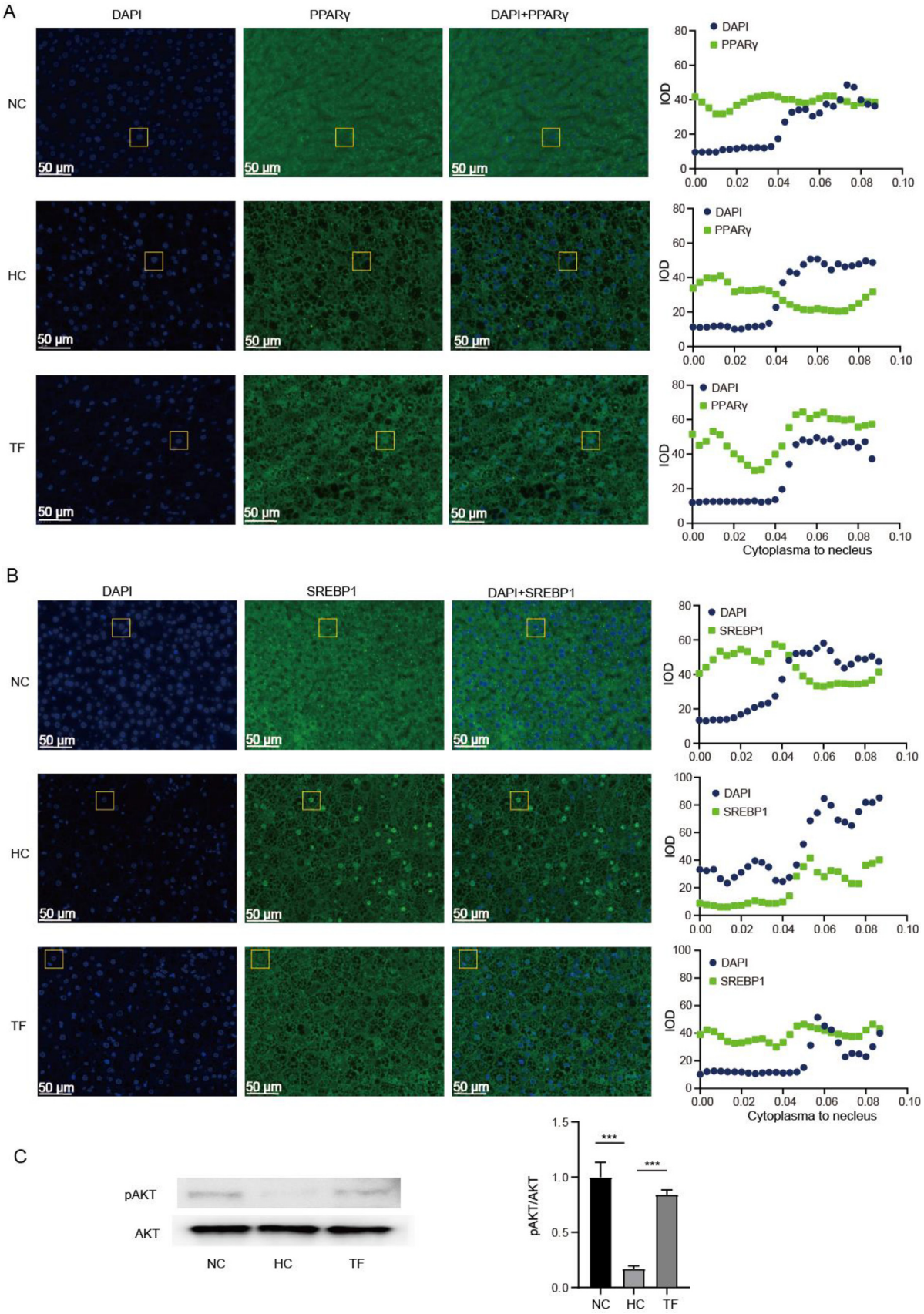

Fig. 5. Effect of TFT on PPARγ, SREBP1, and AKT in HFD-induced rats. A: Immunofluorescence staining for PPARγ in liver tissue (original magnification, ×200). The line chart presents the change in expression in the cytoplasm and nucleus; B: immunofluorescence staining for SREBP1 in liver tissue (original magnification, ×200). The line chart presents the change in expression in the cytoplasm to the nucleus. C: Immunoblotting and densitometric analysis of pAKT/AKT.

3.7. Effect of TFT on hepatic lipid profiles, liver function, and hepatic histomorphology in HFD-induced rats

As shown in Fig. 4A–B, compared with the NC group, the HC group showed significant increases in hepatic TG ($P < 0.001$) and TC ($P < 0.001$). Compared with the HC group, the TF group showed significant decreases in hepatic TC ($P < 0.001$) and TG ($P < 0.001$). As shown in Fig. 4C–D, compared with the NC group, the HC group showed significant increases in plasma ALT ($P < 0.001$) and AST ($P < 0.001$). Compared with the HC diet, the TF group showed decreases in plasma ALT ($P = 0.1077$) and AST ($P = 0.1164$). Furthermore, as shown in Fig. 4E, compared with the NC group, the HC group showed more lipid droplets and irregular morphology, while there were fewer lipid droplets and less irregular morphology in the TF group.

3.8. Effect of TFT on PPARγ, SREBP1 and AKT in HFD-induced rats

As shown in Fig. 5A, compared with the NC group, the HC group showed PPARγ translocation from the nucleus to the cytoplasm. Compared with the HC group, the TF group showed increased PPARγ translocation from the cytoplasm to the nucleus, which indicated that TFT activated the transcriptional activity of PPARγ. As shown in Fig. 5B, compared with the NC group, the HC group showed increased SREBP1 translocation from the cytoplasm to the nucleus. Compared with the HC group, the TF group showed increased SREBP1 translocation from the nucleus to the cytoplasm, which indicated that TFT inhibited the transcriptional activity of SREBP1. As shown in Fig. 5C, compared with the NC group, the HC group showed a significant decrease in AKT ($P < 0.001$) phosphorylation. Compared with the HC group, the TF group showed a significant increase in AKT ($P < 0.001$) phosphorylation.

3.9. Effect of TFT on inflammatory factors and NF-κB in HFD-induced rats

As shown in Fig. 6A–D, compared with the NC group, the HC group showed significant increases in IL6 ($P < 0.001$) and TNFα ($P < 0.001$, $P < 0.01$) in both the plasma and liver. Compared with the HC group, the TF group had significantly reduced hepatic IL6

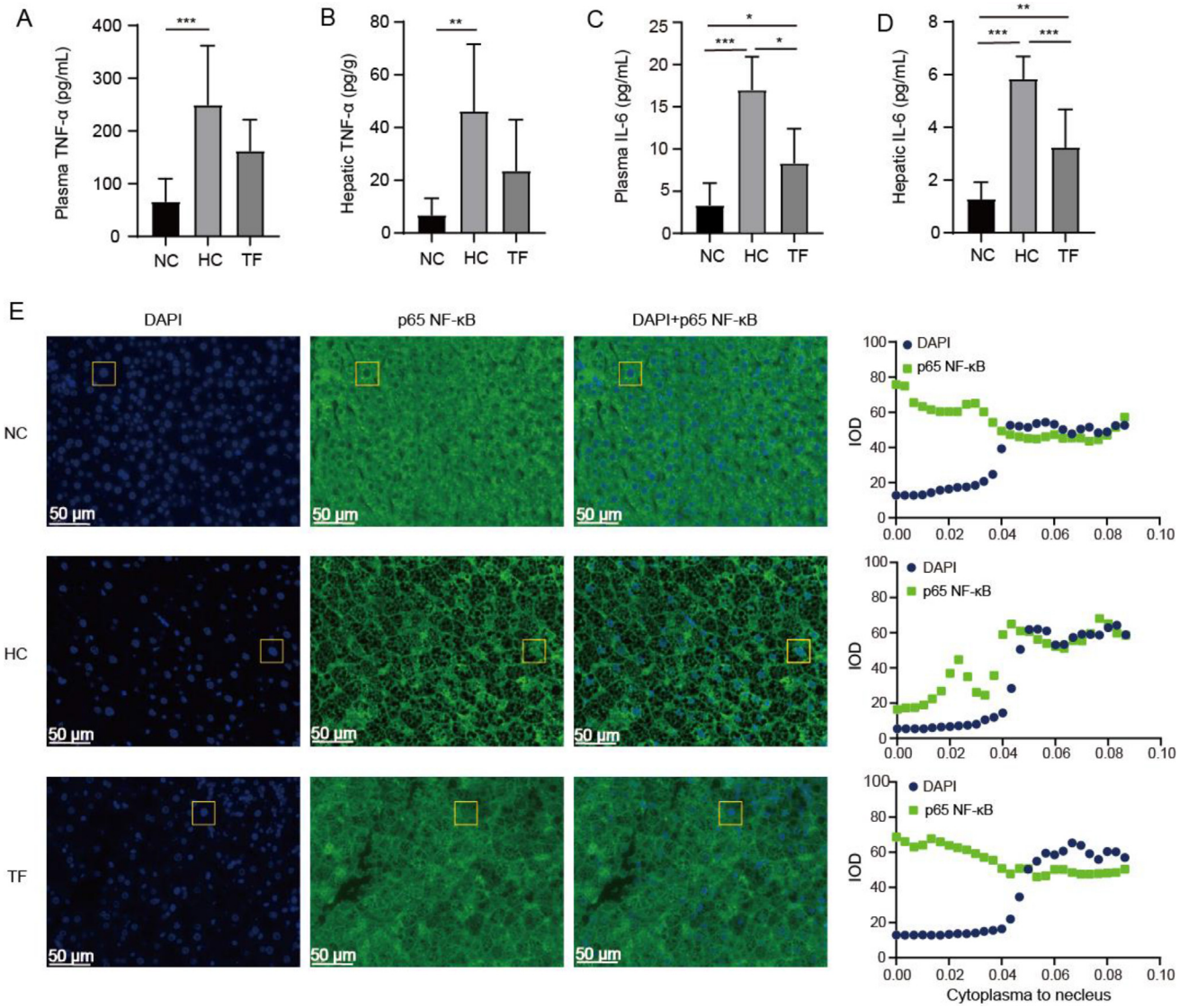

Fig. 6. Effect of TFT on inflammatory factors and NF-κB in HFD-induced rats. A: Hepatic TNF-α; B: plasma TNF-α; C: hepatic IL-6; D: plasma IL-6; E: immunofluorescence staining for p65 NF-κB in liver tissue (original magnification, ×200). The line chart presents the change in expression in the cytoplasm to the nucleus.

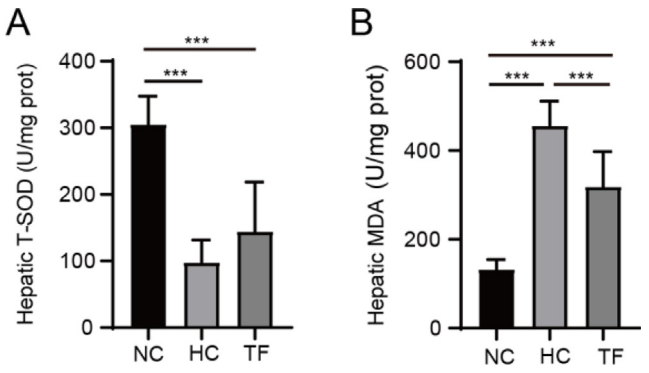

Fig. 7. Effect of TFT on hepatic T-SOD (A) and MDA (B) in HFD-induced rats.

in both the plasma (P < 0.05) and liver (P < 0.001) but little decrease in TNFα in both the plasma (P = 0.0869) and liver (P = 0.0625). As shown in Fig. 6E, compared with the NC group, the HC group showed NF-κB translocation from the cytoplasm to the nucleus. Compared with the HC group, the TF group showed increased NF-κB translocation from the nucleus to the cytoplasm, which indicated that TFT inhibited the transcriptional activity of NF-κB.

3.10. Effect of TFT on hepatic T-SOD and MDA in HFD-induced rats

As shown in Fig. 7A, compared with the NC group, the HC group showed a significant decrease in hepatic T-SOD (P < 0.001). Compared with the HC group, the TF group showed an increase in hepatic T-SOD (P = 0.2117). As shown in Fig. 7B, compared with the NC group, the HC group showed a significant increase in hepatic MDA (P < 0.001). Compared with the HC group, the TF group showed a significant decrease in hepatic MDA (P < 0.001).

4. Discussion

NAFLD is a clinicopathological syndrome characterized by excessive fat deposition in liver cells. In the past 20 years, with tremendous changes in people's lifestyles, NAFLD has become the most common liver disease in the world, but it has not attracted enough attention. The academic community predicts that NAFLD-related advanced liver disease and its mortality, as well as the overall disease burden, will increase significantly (Chris et al., 2018). Therefore, it is urgent to investigate a practical treatment plan. However, due to the complex pathogenesis of NAFLD, there are currently no FDA-approved drugs for NAFLD treatment. Therefore, it is necessary to develop effective and safe medicines or functional foods for preventing and treating NAFLD. At present, Chinese medicine is gradually being recognized worldwide because of its good curative effects and few side effects. TFT has been regarded as a Chinese medicine that courses liver *qi* and resolves depression and might have notable benefits in the treatment of NAFLD. In this study, our results indicated that TFT could prevent and treat NAFLD by reducing lipid accumulation, improving insulin sensitivity, suppressing inflammation, and reducing oxidative stress. Moreover, AKT1, PPARG, SPRBP1, RELA, etc., were confirmed as key targets of TFT in HFD-induced rats.

At present, the "multiple hits" theory is widely accepted to underlie the pathogenesis of NAFLD; this theory states that insulin resistance, adipose tissue dysfunction, mitochondrial dysfunction, endoplasmic reticulum stress, inflammation activation, fatty acids and other factors are involved in the progression of NAFLD (Buzzetti, Pinzani, & Tsochatzis, 2016). In our research, network pharmacology indicated that the targets of TFT are significantly enriched in the AGE-RAGE signalling pathway in diabetic complications (hsa04933), the fluid shear stress and atherosclerosis pathway (hsa05418), the TNF signalling pathway (hsa04668), the IL-17 signalling pathway (hsa04657), and NAFLD (hsa04932). Recent studies have shown that these five pathways are all related to inflammation. The fluid shear stress and atherosclerosis pathway (hsa05418) are related to hepatic lipid metabolism; NAFLD (hsa04932) is related to insulin resistance, and the AGE-RAGE signalling pathway in diabetic complications (hsa04933) is related to oxidative stress. Therefore, these enrichment results showed that the main mechanisms of TFT against NAFLD were inflammation, hepatic lipid metabolism, insulin resistance, and oxidative stress (Liu et al., 2020). Based on the enrichment results, these mechanisms were further analysed.

The most basic feature of nonalcoholic fatty liver is lipid accumulation. Excessive accumulation of lipids will lead to subsequent hepatic lipid peroxidation and inflammation (Ipsen, Lykkesfeldt, & TvedenNyborg, 2018). Therefore, improving liver lipid accumulation is very important for the treatment of NAFLD. Our PPI network indicated that the *SREBP1* gene is a key node in the PPI network and that SREBP1 could regulate FASN and ACC, which are critical for lipid synthesis. Furthermore, our immunofluorescence results show that TFT inhibits the transcription of *SREBP1* in the nucleus, thereby inhibiting the expression of downstream FASN and ACC proteins to inhibit hepatic lipid accumulation (Dan et al., 2017). This inhibition might be one of the main mechanisms by which TFT can treat NAFLD. Previous studies have shown that white chrysanthemum extract could reduce the expression of ACC by regulating SREBP-1c, which supports our results (Tsai et al., 2017). Insulin resistance is also closely related to lipid accumulation. Studies have shown that when insulin resistance increases, it can also lead to an increase in liver lipid accumulation. PPAR-γ, which is encoded by the *PPARG* gene, is closely related to insulin resistance. Thiazolidinediones (TZDs), as PPAR-γ agonists, are a class of agents commonly used for the treatment of patients with type 2 diabetes or insulin resistance. AKT is also closely related to insulin resistance, and the phosphorylation of AKT could increase insulin sensitivity. Our results indicated that AKT1 and PPARG are key nodes in the PPI network and that TFT could increase the phosphorylation of AKT and activate PPAR-γ. Many previous studies have shown that the main compounds from white chrysanthemum could improve insulin resistance by regulating AKT and PPARG (Nishina et al., 2019). Other studies also indicated that flavonoids from Daidaihua and polyphenol extracts of double rose could improve insulin resistance by regulating AKT (Kim, Park, et al., 2012; Liu et al., 2017). These studies are consistent with our results, indicating that TFT might prevent and treat NAFLD by improving insulin resistance.

Inflammation plays a very important role in the development of NAFLD. When lipid peroxidation occurs, it will lead to an inflammatory response and might further lead to apoptosis and cell death, which prevents the reversal of NAFLD. Therefore, inhibiting liver inflammation is an important measure to inhibit the progression from NASL to NASH. The NF-κB family, which is composed of five members, NFKB1, NFKB2, REL, RELA, and RELB, is closely related to inflammation. When p56 NF-κB (encoded by RELA) is activated, it enters the nucleus and causes the cells to produce corresponding inflammatory factors, such as IL-6 and TNF-α, and these two inflammatory factors further cause the corresponding inflammatory response, leading to cell apoptosis. Our results indi-

cated that IL6 and RELA are key nodes and that TFT could inhibit the transfer of p56 NF-κB from the cytoplasm to the nucleus and reduce the level of IL6 in the plasma and liver. Previous studies have also indicated that euscaphic acid from double rose, flavonoids from Daidaihua, and lupeol from white chrysanthemum could inhibit NF-κB transcriptional activity to reduce inflammation (IL-6). These studies have suggested that double rose, white chrysanthemum, and Daidaihua are the main active herbs in TFT that exert anti-inflammatory effects; these findings are very consistent with our results and might be an important mechanism for NAFLD prevention and treatment (Kim, Ryu, et al., 2012; Kang et al., 2011; Kang et al., 2013).

Excessive oxidative stress is also an important pathogenic factor of NAFLD. Excessive oxidative stress levels can cause cell damage and affect liver function. Therefore, improving or reducing oxidative stress is necessary for NAFLD treatment. TFT contains many flavonoids, such as quercetin, cranin, luteolin, diosmetin and naringenin, which are natural antioxidants and can reduce oxidative stress (Schwinn, Markham, & Giveno, 1993). Our results also indicated that TFT could significantly improve the antioxidant biological indicators T-SOD and MDA, indicating that TFT indeed has a strong antioxidant effect, which is helpful for NAFLD treatment and prevention.

NAFLD is also related to intestinal flora and genetic factors, which requires additional research on TFT. Previously, many researchers have reported that many ingredients in TFT might have certain effects on bacteria. For example, white chrysanthemi has a significant inhibitory effect on certain pathogenic bacteria, such as *Enterobacter, Enterococcus, Clostridium* and *Bacteroides*, but has a probiotic effect on *Lactobacillus* and *Bifidobacterium* (Tao et al., 2016). Therefore, TFT might also prevent and treat NAFLD by improving the intestinal flora, although this possibility still requires further research.

The mechanism of TFT against NAFLD has not been determined by systematic studies. Here, our research confirms that TFT can prevent and treat NAFLD through multiple targets. Because of its multitarget characteristics, TFT has advantages over single-target drugs, such as PPAR-γ agonists and antioxidants, and it is more suitable for the treatment of NAFLD. Although TFT has been used for thousands of years, its side effects and whether it is suitable for long-term use still need to be further researched.

5. Conclusion

In summary, TFT could prevent and treat NAFLD by reducing lipid accumulation, improving insulin sensitivity, suppressing inflammation, and reducing oxidative stress. Moreover, AKT1, PPARG, SPRBP1, and RELA were confirmed as the key targets of TFT for NAFLD prevention and treatment. This study also verified the advantages of TCM in dealing with complex pathologies and provided a theoretical basis for elucidating the mechanism of action of TCM. However, this study also has certain shortcomings. Additional targets of TFT for NAFLD prevention and treatment need to be verified, and further clinical trials are needed.

Declaration of Competing Interest

The authors declare that they have no known competing financial interests or personal relationships that could have appeared to influence the work reported in this paper.

Acknowledgements

This research was supported by the fund for the National Natural Science Foundation of China (Grant No. 81903878), the Natural Science Foundation of Shandong Province, China (Grant No. ZR2019BH049), and Major Science and Technology Innovation Project of Shandong Province (Grant No. 2019JZZY020612).

Appendix A. Supplementary data

Supplementary data to this article can be found online at https://doi.org/10.1016/j.chmed.2022.03.002.

References

Amarapurkar, D. N., Hashimoto, E., Lesmana, L. A., Sollano, J. D., Chen, P. J., & Goh, K. L. (2007). How common is non-alcoholic fatty liver disease in the Asia-Pacific region and are there local differences. *Journal of Gastroenterology and Hepatology, 22*(6), 788–793.

Adler, M., & Schaffner, F. (1979). Fatty liver hepatitis and cirrhosis in obese patients. *The American Journal of Medicine, 67*(5), 811–816.

Buzzetti, E., Pinzani, M., & Tsochatzis, E. A. (2016). The multiple-hit pathogenesis of non-alcoholic fatty liver disease (NAFLD). *Metabolism, 65*(8), 1038–1048.

Caldwell, S. H., Argo, C. K., & Alosaimi, A. M. S. (2006). Therapy of NAFLD: Insulin sensitizing agents. *Journal of Clinical Gastroenterology, 40*, 61–66.

Chen, Y. C. (2012). TCM Database@Taiwan: The World's Largest Traditional Chinese Medicine database for drug screening in silico. *PLoS One, 6*(1) e15939.

Chris, E., Homie, R., Rohit, L., Zobair, Y., & Sanyal, A. J. (2018). Modeling the epidemic of nonalcoholic fatty liver disease demonstrates an exponential increase in burden of disease. *Hepatology, 67*(1), 123–133.

Dan, L., Xiao, H., Dong, J., Yuan, L., & Fa, N. S. (2017). B7–H3 regulates lipid metabolism of lung cancer through SREBP1-mediated expression of FASN. *Biochemical and Biophysical Research Communications, 482*(4), 1246–1251.

Friedman, S. L., Neuschwander-Tetri, B. A., Mary, R., & Sanyal, A. J. (2018). Mechanisms of NAFLD development and therapeutic strategies. *Nature Medicine, 24*(7), 908–922.

Gierke, P., Zhao, C., Brackmann, M., Linke, B., Heinemann, U., & Braunewell, K. H. (2004). Expression analysis of members of the neuronal calcium sensor protein family: Combining bioinformatics and Western blot analysis. *Biochemical and Biophysical Research Communications, 323*(1), 38–43.

Hopkins, A. (2008). Network pharmacology: The next paradigm in drug discovery. *Nature Chemical Biology, 4*, 682–690.

Harry, E. J., Pogliano, K., & Losick, R. (1995). Use of immunofluorescence to visualize cell-specificgene expression during sporulation in *Bacillus subtilis*. *Journal of Bacteriology, 177*(12), 3386–3393.

Ipsen, D. H., Lykkesfeldt, J., & TvedenNyborg, P. (2018). Molecular mechanisms of hepatic lipid accumulation in non-alcoholic fatty liver disease. *Cellular and Molecular Life Sciences, 75*(18), 3313–3327.

Kumar, R. (2013). Hard clinical outcomes in patients with NAFLD. *Hepatology International, 7*(2), 790–799.

Kou, J., Zhu, D., & Yan, Y. (2005). Neuroprotective effects of the aqueous extract of the Chinese medicine Danggui-Shaoyao-san on aged mice. *Journal of Ethnopharmacology, 97*(2), 313–318.

Kim, G. S., Park, H. J., Woo, J. H., Kim, M. K., Koh, P. O., Min, W., ... Cho, J. H. (2012a). *Citrus aurantium* flavonoids inhibit adipogenesis through the Akt pathway in 3T3-L1 cells. *BMC Complementary and Alternative Medicine, 12*(1), 31.

Kim, I. T., Ryu, S., Shin, J. S., Choi, J. H., Park, H. J., & Lee, K. T. (2012b). Euscaphic acid isolated from roots of *Rosa rugosa* inhibits LPS-induced inflammatory responses via TLR4-mediated NF-κB inactivation in RAW 264.7 macrophages. *Journal of Cellular Biochemistry, 113*(6), 1936–1946.

Kang, S. R., Park, K. I., Park, H. S., Lee, D. H., Jin, A. K., Nagappan, A., ... Park, M. K. (2011). Anti-inflammatory effect of flavonoids isolated from Korea *Citrus aurantium* L. on lipopolysaccharide-induced mouse macrophage RAW 264.7 cells by blocking of nuclear factor-kappa B (NF-κB) and mitogen-activated protein kinase (MAPK) signalling pathways. *Food Chemistry, 129*(4), 1721–1728.

Kang, S. C., Lim, S. Y., & Song, Y. J. (2013). Lupeol is one of active components in the extract of *Chrysanthemum indicum* Linne that inhibits LMP1-induced NF-κB activation. *PLoS One, 8*(11) e82688.

Liu, J., Lin, B., Chen, Z., Deng, M., Wang, Y., Wang, J., ... Chen, C. (2020). Identification of key pathways and genes in nonalcoholicfatty liver disease using bioinformatics analysis. *Archives of Medical Science, 16*(2), 374–385.

Liu, L., Tang, D., Zha, O. H., Xin, X., & Aisa, H. A. (2017). Hypoglycemic effect of the polyphenols rich extract from *Rose rugosa* Thunb on high fat diet and STZ induced diabetic rats. *Journal of Ethnopharmacology, 200*, 174–181.

Marrero, J. A., Fontana, R. J., Su, G. L., Conjeevaram, H. S., Emick, D. M., & Lok, A. S. (2002). NAFLD may be a common underlying liver disease in patients with hepatocellular carcinoma in the United States. *Hepatology, 36*(6), 1349–1354.

Mavrevski, R., Traykov, M., Trenchev, I., & Trencheva, M. (2018). Approaches to modeling of biological experimental data with Graphpad prism software. *WSEAS Transactions on Systems and Control, 13*, 242–247.

Nandi, D., Patra, R. C., & Swarup, D. (2006). Oxidative stress indices and plasma biochemical parameters during oral exposure to arsenic in rats. *Food and Chemical Toxicology, 44*(9), 1579–1584.

Nishina, A., Sato, D., Yamamoto, J., Kobayashi-Hattori, K., & Hirai, Y. (2019). Antidiabetic-like effects of naringenin-7-*O*-glucosidefrom edible *Chrysanthemum* 'Kotobuki' and naringenin by activation of the PI3K/Akt pathway and PPARγ. *Chemistry & Biodiversity, 16*(1) e1800434.

Rinella, M., & Sanyal, A. (2015). Genetics, diagnostics and therapeutic advances in NAFLD. *Nature Reviews Gastroenterology and Hepatology, 12*, 65–66.
Schwinn, K. E., Markham, K. R., & Giveno, N. K. (1993). Floral flavonoids and the potential for pelargonidin biosynthesis in commercial *Chrysanthemum cultivars*. *Phytochemistry, 5*(1), 145–150.
Thoma, C., Day, C. P., & Trenell, M. I. (2012). Lifestyle interventions for the treatment of non-alcoholic fatty liver disease in adults: A systematic review. *Journal of Hepatology, 56*(1), 255–266.
Tsai, P. J., Chang, M. L., Hsin, C. M., Chuang, C. C., & Wu, W. H. (2017). Antilipotoxicity activity of *Osmanthus fragrans* and *Chrysanthemum morifolium* flower extracts in hepatocytes and renal glomerular mesangial cells. *Mediators of Inflammation, 2017*(23), 1–12.
Tao, J. H., Duan, J. A., Qian, Y. Y., Qian, D. W., & Guo, J. M. (2016). Investigation of the interactions between *Chrysanthemum morifolium* flowers extract and intestinal bacteria from human and rat. *Biomedical Chromatography, 30*(11), 1807–1819.
Woods, S. C., Seeley, R. J., Rushing, P. A., Alessio, D. D., & Tso, P. (2003). A controlled high-fat diet induces an obese syndrome in rats. *The Journal of Nutrition, 133*(4), 1081–10877.